HIGHLIGHT

Liquid Crystalline Conjugated Polymers and Their Applications in Organic Electronics

SHENG-HSIUNG YANG, CHAIN-SHU HSU
Department of Applied Chemistry, National Chiao Tung University,
1001 Ta-Hsueh Road, Hsinchu 30010, Taiwan, Republic of China

Received 23 January 2009; Accepted 30 January 2009
DOI: 10.1002/pola.23342
Published online in Wiley InterScience (www.interscience.wiley.com).

ABSTRACT: This article describes the syntheses and electro-optical applications of liquid crystalline (LC) conjugated polymers, for example, poly(*p*-phenylene vinylene), polyfluorene, polythiophene, and other conjugated polymers. The polymerization involves several mechanisms: the Gilch route, Heck coupling, or Knoevenagel condensation for poly(*p*-phenylenevinylene)s, the Suzuki- or Yamamoto-coupling reaction for polyfluorenes, and miscellaneous coupling reactions for other conjugated polymers. These LC conjugated polymers are classified into two types: conjugated main chain polymers with long alkyl side chains, namely main-chain type LC polymers, and conjugated polymers grafting with mesogenic side groups, namely side-chain type LC conjugated polymers. In general, the former shows higher transition temperature and only nematic phase; the latter possesses lower transition temperature and more mesophases, for example, smectic and nematic phases, depending on the structure of mesogenic side chains. The fully conjugated main chain promises them as good candidates for polarized electroluminescent or field-effect devices. The polarized emission can be obtained by surface rubbing or thermal annealing in liquid crystalline phase, with maximum dichroic ratio more than 20. In addition, conjugated oligomers with LC properties are also included and discussed in this article. Several oligo-fluorene derivatives show outstanding polarized emission properties and potential use in LCD backlight application. © 2009 Wiley Periodicals, Inc. J Polym Sci Part A: Polym Chem 47: 2713–2733, 2009

Keywords: conducting polymers; conjugated polymers; field effect transistor; light-emitting diodes; liquid crystalline; liquid-crystalline polymers (LCP); polarized electroluminescence; polyfluorene; poly(*p*-phenylenevinylene); polythiophene

Correspondence to: C.-S. Hsu (E-mail: cshsu@mail.nctu.edu.tw)

Journal of Polymer Science: Part A: Polymer Chemistry, Vol. 47, 2713–2733 (2009)

S. H. YANG

S. H. Yang received his B.S. degree in Department of Applied Chemistry in 1998 from National Chiao Tung University, Taiwan. He obtained his Ph.D. degree in material science from University of Nantes, France in 2004. His research interests include liquid crystalline polymers, organic light-emitting diodes, and self-assembly of conjugated materials. Currently, he is a postdoctoral researcher on light-emitting polymers in Prof. Chain-Shu Hsu's laboratory.

CHAIN-SHU HSU

Chain-Shu Hsu received his Ph.D. from Case Western Reserve University in 1987 and did his postdoctoral work at National Tsing Hua University in Taiwan. He joined the Department of Applied Chemistry of the National Chiao Tung University, Taiwan in 1988 as an associate professor and was promoted to full professor in 1991. Currently, he is serving as a vice president and chair professor of the National Chiao Tung University. His research interests include liquid crystalline polymers and conjugated polymers, polymer light-emitting diodes, and organic photovoltaics. He has published more than 160 research papers and 18 patents. He is currently in the international advisory boards of *Polymer* and Editorial boards of *Journal of Polymer Science: Polymer Chemistry*, and *Journal of Polymer Research*. He received the Excellent Research Award of National Science Council, Taiwan in 1994, Franco-Taiwan Scientific Award on nanomaterials in 2006, Teco and Hou Chin Tui Awards in 2007, and Academic Award of the Ministry of Education, Taiwan in 2008.

INTRODUCTION

Liquid crystalline (LC) materials have large anisotropy of optical, electrical, magnetic, and physical properties because of their anisotropy molecular structure and molecular alignment. They can show a variety of characteristic behavior on application of electric and magnetic fields. On the other hand, conjugated polymers with highly extended π-conjugation in their main chain have attracted considerable attention from both fundamental and practical points of view, because various novel physical behaviors have been observed and also various functional applications have been proposed.[1–4] Recently, a variety of LC conjugated polymers having a mesogenic part in their side-chain or long alkoxy side-chains as a substituent were synthesized and characterized. Such kinds of new conjugated polymers can be aligned under LC phase and used for the application of polarized electroluminescence (EL) devices and organic thin film transistors.

LC conjugated polymers have been a subject of two review articles. In 2001, Neher reviewed the LC polyfluorene homopolymer for bright blue emission and polarized EL.[5] In 2003, Lam and Tang reviewed the LC polyacetylenes.[6] In this highlight, we will avoid duplication with two previous reviews. We will concentrate on LC poly(*p*-phenylenevinylene) (LC PPV), LC polyfluorene (LC PF), and side-chain LC conjugated polymers. The LC polyfluorene will be covered by only those publications after 2001.

LC POLY(*P*-PHENYLENEVINYLENE)

For the development of conducting and luminescent polymers, the fully conjugated polymer PPV and its derivatives have attracted a great deal of attention because of their particular structures and highly interesting opto-electrical properties. Many synthetic routes have been proposed and widely used to prepare PPV derivatives, including Wessling and Zimmerman route,[7] Gilch route,[8] chlorine precursor route,[9] Heck coupling polymerization,[10] Wittig condensation,[11] and Knoevenagel polycondensation.[12] Because long alkyl chains or mesogenic groups are incorporated onto the monomer structure before polymerization, the forming polymers are usually soluble in common organic solvents. This feature simplifies the synthetic procedure, that is, no

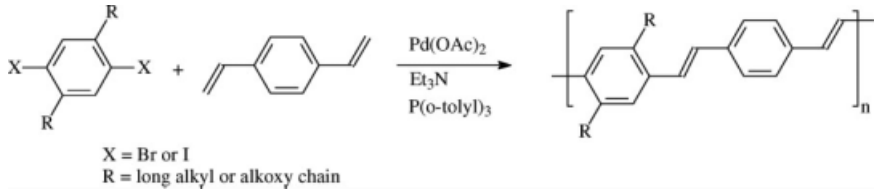

Scheme 1. Synthesis of PPVs via Heck coupling polymerization.

thermal conversion process is required for the preparation of these polymers, which possess intrinsic solubilities in many solvents.

The *trans*-PPV backbone is a rigid rod that can act as the mesogenic unit. Those alkyl or alkoxy side chains attached to the phenyl ring of the main chain are regarded as soft spacers, resulting in so-called "hairy-rod" polymers.[10,13,14] The solubility of these LC PPVs in common organic solvents is highly improved by alkyl/alkoxy side chains. Before 2000, Heck coupling polymerization was mostly applied to synthesize LC PPV derivatives. In a typical Heck coupling polymerization, an aromatic dihalide and a divinylbenzene are coupled to generate fully conjugated main chain, as shown in Scheme 1. The molecular weights of obtained polymers are not very high (usually below 30,000 KDa), and the polydispersity index (PDI) values are often larger than 2. Besides, the removal of palladium catalysts is essentially required to reach better performance of their EL devices.

To examine the LC properties of certain materials, polarized optical microscopy (POM) provides fast and supplemental observation of the transitions. Polymers that show birefringent fluids under cross polarization above the melting temperatures are regarded to possess LC properties. Most LC PPV derivatives show nematic texture under their LC state (**P1** in Chart 1).[10] The texture is reversible at a slower cooling rate of 1–5 °C/min, because polymers own higher viscosity compared with small molecules. The high molecular weight of conjugated polymers makes it difficult to grow the characteristic Schlieren textures exhibited by small molecule nematic liquid crystals. The authors also found that the melting and clearing transition temperatures are affected by the lengths of the side chains. As the carbon number of the side chain increases from 4 to 12, both melting and clearing temperatures decrease steadily.

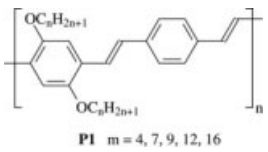

Chart 1. Dialkoxy-PPV.

The substitution on the aromatic ring can be long alkyl or alkoxy chains, usually longer than hexyl group ($C > 6$). Such kind of PPV derivatives can show LC properties, usually nematic texture under cross polarization; the LC temperature range of those polymers is also pretty wide, about 80–100 °C. In addition to dialkylated PPV derivatives, PPVs with dendritic side chains were also reported to have LC properties (**P2** and **P3** in Chart 2).[15] Different generations of polyaryl ether dendrons (e.g., Fréchet-type dendrons) were attached onto PPV main chain, and their LC phases were verified by POM and X-ray diffraction technique. Figure 1 shows X-ray diffraction patterns and optical photographs of dendron-containing **P2** and **P3**, both exhibiting thermotropic nematic mesophase. The nematic-to-isotropic transition temperature was measured to be 200 ± 5 °C for **P2** and 211 ± 5 °C for **P3**. The nematic character of these PPV derivatives can be exploited to generate strongly aligned films, resulting in enhanced photoconductivity and better charge transport capability, as well as polarized light emission.

From 2000, the Gilch route is widely used to prepare soluble PPV derivatives, including LC ones. The Gilch route employs α,α′-dihalo-*p*-xylene with excess base, usually *tert*-BuOK in organic solvents. Alkyl or alkoxy chains are also incorporated onto the aromatic rings before polymerization to improve the solubility of the resulting polymers. A typical Gilch route to solution-processible PPV derivatives is depicted in Scheme 2. The polymerization condition is mild and the molecular weights of obtained polymers are relatively large. In

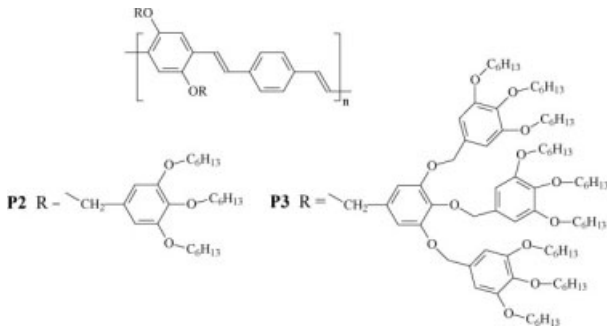

Chart 2. PPV with dendritic side chains.

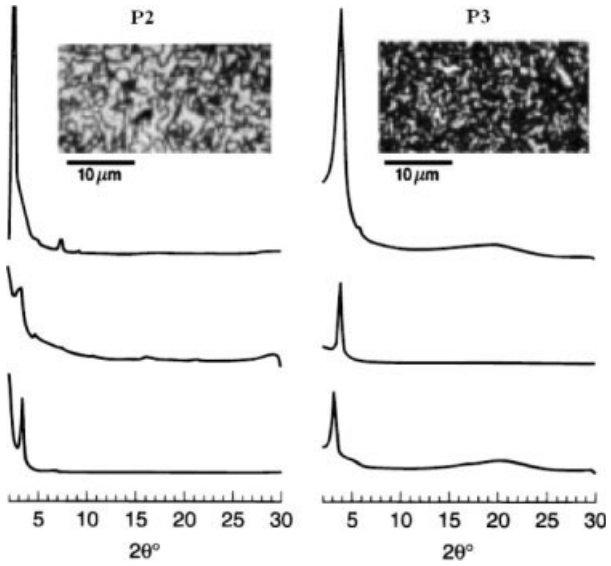

Figure 1. Optical textures and WAXS patterns of polymers **P2** and **P3**.

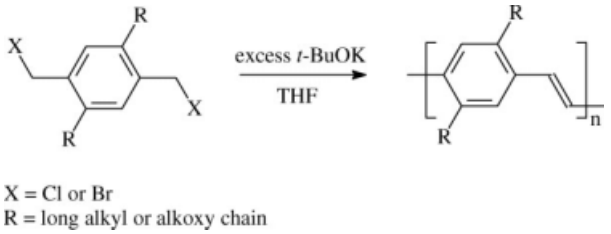

Scheme 2. Synthesis of PPVs via Gilch route.

some cases, gelation or precipitation of polymeric products may occur during polymerization. Neef and Ferraris[8] proposed a general synthetic method to carry out the Gilch route by reversed addition of base and using 4-methoxyphenol as an end-capping agent to prepare poly(2-methoxy-5-(2′-ethylhexyloxy)-1,4-phenylenevinylene) (MEH-PPV).

Several disubstituted PPV derivatives, including MEH-PPV,[16] poly(2,5-dioctyloxy-1,4-phenylenevinylene) (DO-PPV),[17] and poly(2,5,2′,5′-tetrahexyloxy-8,7′-dicyano-di-*p*-phenylenevinylene) (DH-CNPPV),[18] are found to exhibit nematic-like optical texture. Su et al. demonstrated that these light-emitting conjugated polymers are mesomorphic in nature, showing nematic-like texture under cross polarization. Combining with the observations of X-ray diffraction and transmission electron microscopy (TEM), these hairy-rod polymers are confirmed to have supramolecular assembly in general. Figure 2 shows the X-ray diffraction patterns and TEM bright field image for thin specimens annealed at 200 °C, where the lamellar mesophase is fully developed as judged from its X-ray diffraction results. The most prominent morphological feature here is the abundance of worm-like entities ~200 nm in length and 10–20 nm in width. A closer examination indicates that each of these worms is composed of a string of beads 10–20 nm in size.

The lamellar structure was found to be 1.6, 1.8, and 2.0 nm in layer spacing for MEH-PPV, DO-PPV, and DH-CNPPV, respectively. Figure 3 depicts a schematic model connecting the lamellar mesophase in the molecular level to agglomerated worm-like morphology of these conjugated polymers. In their model, the polymer beads (~10–20 nm in size from TEM) are weakly attracted side-by-side in the transverse direction to give worm-like features. Upon shear at an elevated temperature, the worm-like textures are disintegrated into units of beads, within which polymer backbones and the lamellar assemblies are aligned in the shear direction. These beads subsequently reagglomerate into new worm-like entities whose long axes lie perpendicular to the shear direction, with polymer backbones and lamellae lying parallel to the shear direction. The difference among these three polymers is that DO-PPV and DH-CNPPV show the

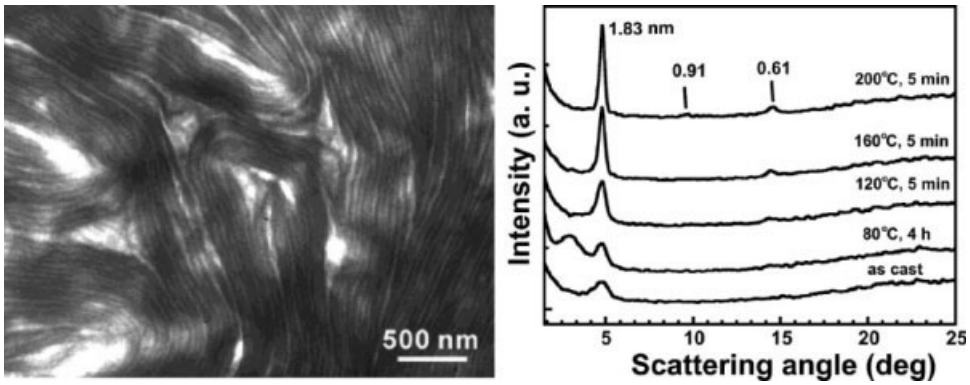

Figure 2. TEM bright-field image of DO-PPV film annealed at 200 °C for 5 min followed by fast cooling to room temperature.

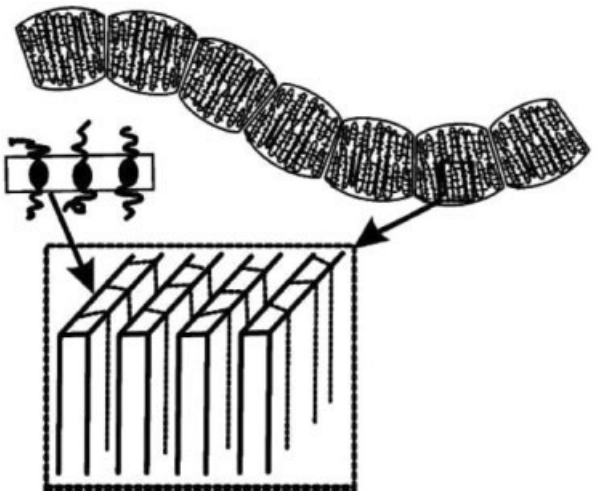

Figure 3. Schematic prepresentation of hierarchical features of polymer aggregates.

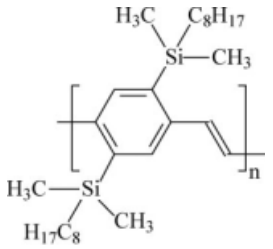

P4

Chart 3. Dioctylsilyl-PPV.

formation of a lamellar mesophase in bulk, whereas MEH-PPV has biaxial nematicity.

A silyl-disubstituted PPV derivative poly[2,5-bis-(dimethyloctylsilyl)-1,4-phenylenevinylene] (**P4** in Chart 3) was reported to have LC properties and polarized emission.[19] From DSC thermogram, two endotherms at 143 and 220 °C were observed, which correspond to melting and isotropization temperature of the polymer, respectively. This polymer has a high PL quantum efficiency of 60% in thin film state. The authors attributed such high PL quantum efficiency to the efficient confinement of the excitons in the main chains and also the molecular ordering effects from its LC properties.

In 1997, Hsieh and coworkers[9] proposed a synthetic route to poly(2,3-diphenyl-1,4-phenylenevinylene) (DP-PPV), which exhibits high photoluminescence (PL) efficiency in the solid state. Different substituents can be introduced on the 5-position of the phenyl ring to improve its properties. By following this synthetic route, monomers containing diversified functional groups are easily synthesized and therefore soluble DP-PPV derivatives with high molecular weights are also easily obtained. For instance, different alkyl side chains from pentyl to decyl groups were incorporated.[20] The resulting polymers show characteristic nematic texture under cross polarization at different temperature, depending on the varieties of the side group. A general route to the notable DP-PPV derivatives is depicted in Scheme 3. In this DPn-PPV series, where n is the carbon number of the alkyl side chain on C-5 position of the phenyl ring, similar nematic texture is found for $n = 5$–10. It is noted that no liquid crystalline phase is observed when the alkyl side chain on C-5 position is too short, for example, a butyl group ($n = 4$). A typical optical texture of DP6-PPV under its mesophase is shown in Figure 4.

All the polymers mentioned above show nematic phase, whereas main-chain conjugated polymers that have smectic phases are relatively rare. Low polydispersed poly(2,5-di(2′-ethylhexyloxy)-1,4-phenylenevinylene) (DEH-PPV) is one example of LC conjugated

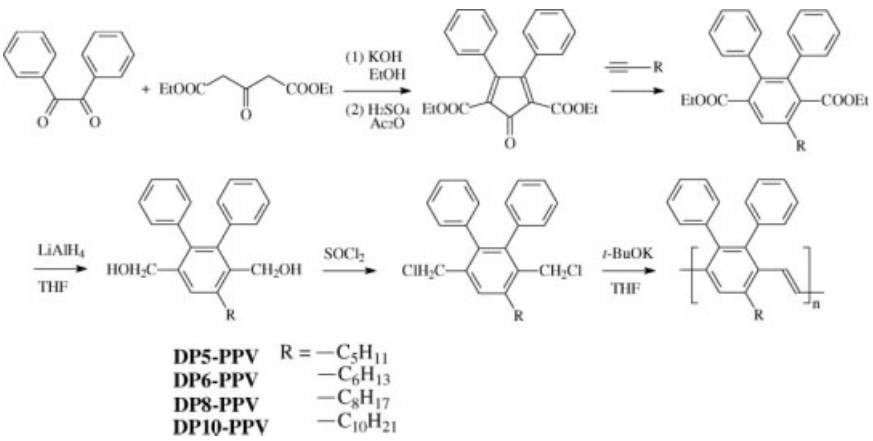

Scheme 3. Synthesis of DP-PPV derivatives containing different side chains.

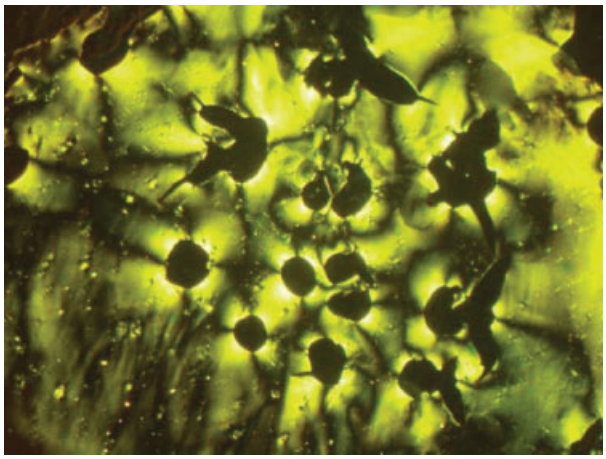

Figure 4. Optical texture of DP6-PPV at 150 °C.

polymers having smectic phase (see Chart 4).[21] The polydispersities of the prepared DEH-PPV were ranged from 1.06 to 1.19, determined by gel permeation chromatography using monodispersed polystyrene as the standard. A typical smectic texture of DEH-PPV at 180 °C is shown in Figure 5. Further heating results in a transition from a smectic to a nematic phase. Low polydispersity is critical to the formation of smectic phases because disorder in chain length disrupts the formation of a single layer thickness. Besides, low molecular weight of synthesized DEH-PPV (M_n values from 4,400 to 10,900) is also responsible for the formation of smectic phase. The molecular weights of previous PPV derivatives are usually pretty high, with M_n value over 20 KDa; the hindrance caused by conjugated main chain is too large to form ordered layer structure. Direct structural evidence in support of LC DEH-PPV is obtained by X-ray scattering. Figure 6 shows the wide-angle X-ray scattering (WAXS) patterns of DEH-PPV with M_n value of 4600, which exhibits crystalline, smectic, and nematic phases upon increasing temperatures. Heating the sample into the smectic phase causes four peaks to develop, and melting to the nematic phase results in decrease in the peak intensity as the material loses order.

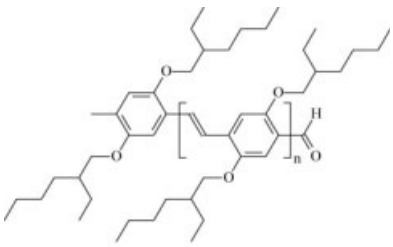

DEH-PPV

Chart 4. Diethylhexyloxy-PPV.

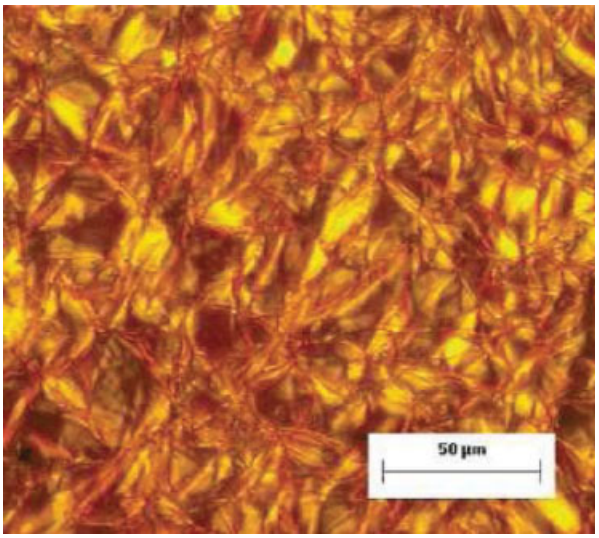

Figure 5. Optical texture of DEH-PPV at 180 °C.

LC POLYFLUORENE

In addition to PPV, polyfluorene (PF) and its derivatives have also drawn a great deal of research interest for their particular structure and emission properties. Two synthetic routes are used to prepare PF derivatives, Suzuki-coupling and Yamamoto-coupling reactions. These two coupling reactions have diverse catalysts and polymerization conditions. In a typical Suzuki-coupling reaction, palladium complex, such as $Pd(PPh_3)_4$, is used as a catalyst to carry out the polymerization in the presence of

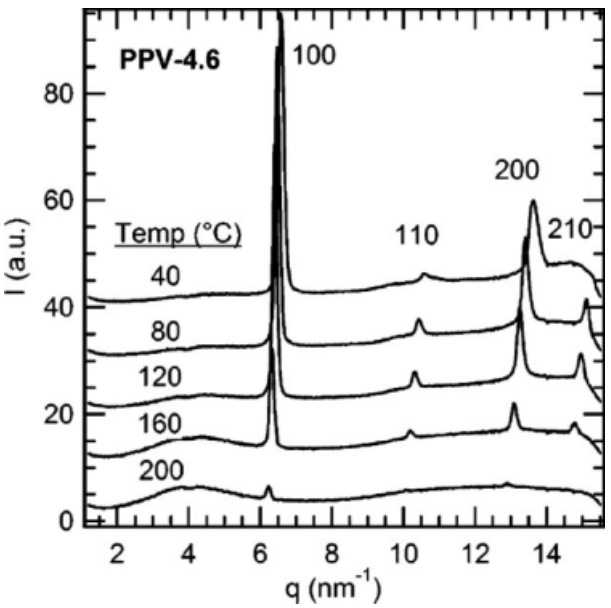

Figure 6. WAXS patterns of DEH-PPV at different temperatures.

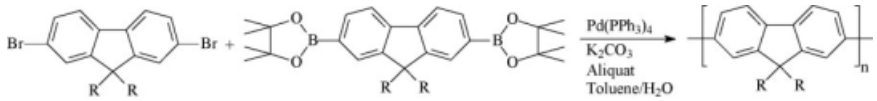

R = long or branched alkyl chain

Scheme 4. Synthesis of PFs via Suzuki-coupling reaction.

K_2CO_3 and a phase transfer catalyst aliquat 336 in a solvent mixture (toluene/degassed water).[22] During polymerization process, dibromofluorene and fluorenylboronic ester react with each other to give PF products; well-defined alternating copolymer can be obtained via Suzuki-coupling polymerization. The molecular weights of obtained PF derivatives are moderate (M_n 10,000–50,000) with low PDI values. A general Suzuki-coupling reaction is given in Scheme 4.

In a typical Yamamoto-coupling reaction, nickel complex, such as $Ni(COD)_2$, is used as catalyst to carry out the polymerization in the presence of cyclooctadiene and cocatalyst 2,2′-bipyridyl in a solvent mixture (toluene/DMF).[23] Corresponding 2,7-dibromofluorene serves as the monomer. This method allows preparation of PF derivatives with very high molecular weight (M_n up to 250,000), which is usually much higher than that made by Suzuki-coupling reaction. However, there are some drawbacks. The amount of nickel complex is relatively large (when compared with palladium complex by Suzuki-coupling reaction) and requires a special work-up to be removed completely. Moreover, the PDI value is usually higher. A general Yamamoto-coupling reaction is given in Scheme 5.

Similar to PPVs, polycyclic aromatic rings of PF main chain can also serve as the mesogenic unit. Long and/or branched alkyl chains incorporated on the C-9 position of fluorene act as soft spacers. Thus, PFs can also be regarded as "hairy-rod" polymers. Neher has reviewed a number of LC PF homopolymers for their blue emission and polarized electrominesescence.[5] Although poly(9,9-dihexylfluorene) (PFH) is generally considered as amorphous, PFs with longer alkyl side chains, for example, poly(9,9-dioctylfluorene) (PFO in Chart 5) or poly(9,9-bis(2-ethylhexyl)fluorene) (PF2/6 in Chart 5), show LC behavior and potential application in polarized PLEDs. The phase behavior of PFO is quite complex, which includes amorphous, nematic, and β phases.[24] Selective formation of three phases can be achieved via judicious choice of process parameter. The amorphous state of PFO is obtained by quick evaporation of solvent, whereas slow solvent removal during film formation or extended treatment of the amorphous film with solvent vapor, that is, solvent annealing, results in predominately β phase. The nematic phase is just in between amorphous and β phase. The conjugation length of PFO under both nematic and β phase is greater than that of the amorphous film. Figure 7 shows the nematic phase of PFO with characteristic schlieren texture under cross polarization. Recently, PFH has been re-verified to exhibit a mesophoric β phase with a layer spacing of $\sim$1.4 nm.[25] The β phase of PFH is inherently metastable and, upon heating above 175 °C, transforms into a crystalline form that melts into a nematic phase above 250 °C. In addition to PF homopolymers, PF copolymers containing different aromatic moieties also show LC properties. The annealed film of poly(9,9-dioctylfluorene-*alt*-thieno[3,2-*b*]thiophene) (PFTT in Chart 6) exhibits a birefringent fluid phase under cross polarization, indicative of its thermotropic nematic liquid crystallinity.[26] Figure 8 shows a crystallization exothermal peak (T_{Cr}) and a melting endothermal peak ($T_{Cr\text{-}LC}$) appeared at 161 and 243 °C, respectively. These characteristic temperatures of PFTT are around 100 °C higher than those previously reported for the corresponding homopolymer PFO, probably because of the introduction of the unsubstituted and rigid thieno[3,2-*b*]thiophene moiety. Poly(9,9-dioctylfluorene-*alt*- bithiophene) (PFT2 in Chart 6) shows similar phase transition and LC behavior.

A PF-triphenylamine (TPA) copolymer (**P5** in Chart 7) synthesized by our group also revealed a schlieren

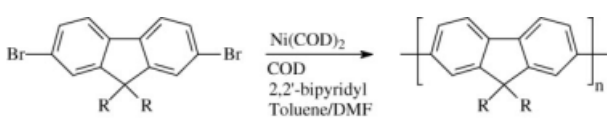

R = long or branched alkyl chain

Scheme 5. Synthesis of PFs via Yamamoto-coupling reaction.

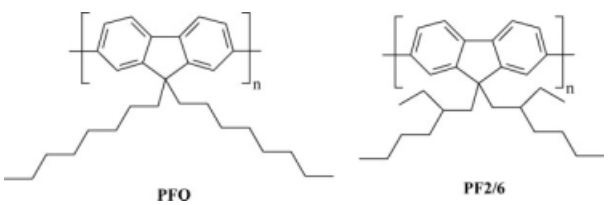

Chart 5. Poly(9,9-dialkylfluorene).

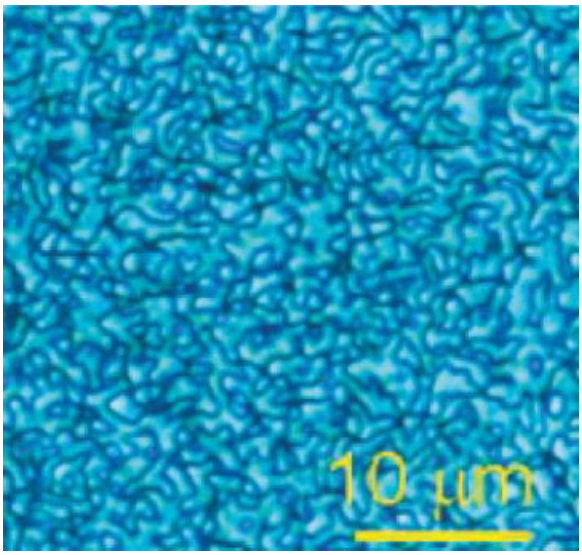

Figure 7. Schlieren-like texture of PFO under LC state.

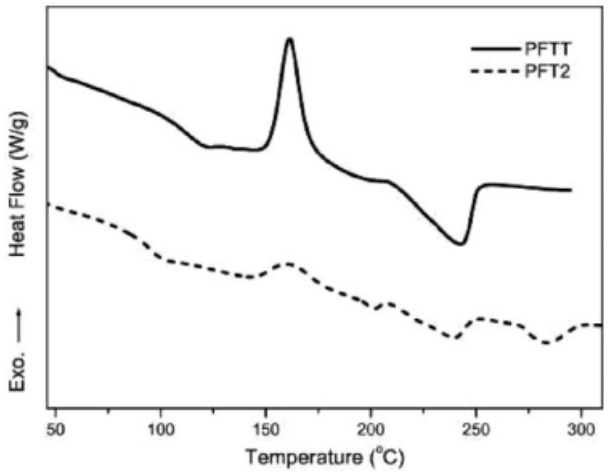

Figure 8. DSC thermograms of polymers PFTT and PFT2.

texture over 100 °C,[27] indicative of a thermotropic nematic liquid crystalline phase (as shown in Fig. 9).

The thermotropic LC properties of fluorene-selenophene-based copolymer (**P6** in Chart 8) were also directly observed by POM.[28] The cast pristine film of the polymer did not exhibit birefringence because of its amorphous phase, whereas the film annealed to 270 °C produced a clear birefringent image because of the LC domains, which is consistent with the phase transition characteristics revealed by the DSC analysis (as shown in Fig. 10). Moreover, the film maintained its birefringence image after quick cooling to room temperature.

Other hairy-rod LC conjugated polymers include polythiophene (PT),[29–31] poly(*p*-phenyleneethynylene) (PPE),[32,33] and poly(*p*-phenylenebutadiynylene) (PPB).[34–36] For these polymers, conjugated backbones backbone serve as rigid mesogenic core, and alkylated side chains on phenyl or thiophene rings help increase solubilities in organic solvents and form LC properties, similar to PPV and PF. The LC properties of these conjugated polymers are mostly examined by POM, DSC and X-ray diffraction experiments, showing nematic phase in their LC range. Typical structures of PT, PPE, and PPB with alkyl side chains are shown in Chart 9.

SIDE-CHAIN LC CONJUGATED POLYMERS

Apart from hairy-rod LC conjugated polymers substituted by flexible aliphatic side chains, introducing mesogenic groups onto π-conjugated main chain has also drawn a lot of research interests. These side chain substituted conjugated polymers have a mesogenic structure similar to traditional side chain LC polymers, such as polyester and polyamide; therefore, they are able to manifest LC properties. The introduction of LC groups has been demonstrated to afford optical dichroism and electrical anisotropies, giving rise to advanced LC conjugated polymers. In 2003, Lam and Tang[6] have reviewed a great number of LC polyacetylene (PA) derivatives containing mesogenic groups. They demonstrated that PAs with mesogenic pendants can be highly emissive with photoluminescent quantum yield of up to 98% and EL performance comparable to some best blue-light-emitting polymers. These sheet-like side chain LC PAs can form monolayer lamellae in dilute solution.[37] The mono-substituted PAs bearing ferroelectric LC groups can also show chiral nematic and smectic phases under LC state.[38] In addition to PAs, many other conjugated

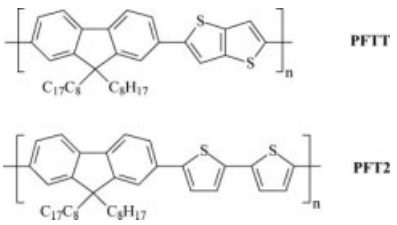

Chart 6. Fluorene-thiophene copolymers.

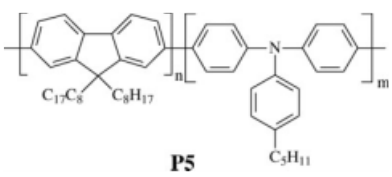

Chart 7. Fluorene-TPA copolymer.

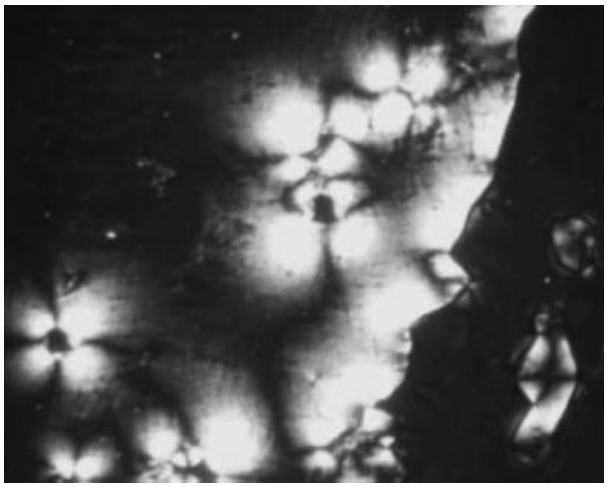

Figure 9. Optical texture of polymer **P5** at 175 °C.

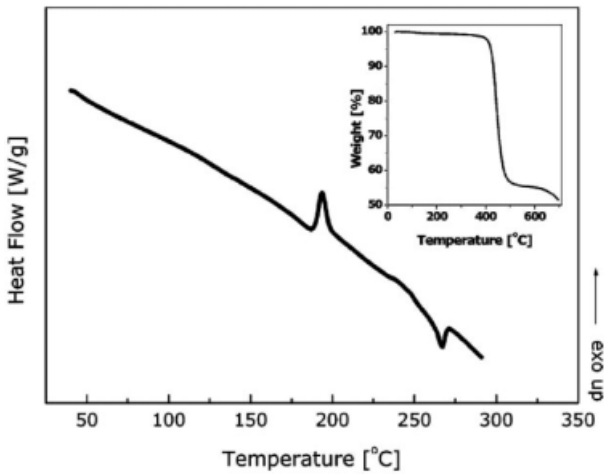

Figure 10. DSC thermogram of polymer **P6** (inset: TGA curve of **P6**).

polymers incorporating with LC side groups have also been synthesized and characterized. Akagi and coworkers[39] synthesized a number of LC polyarylenes and polyarylenevinylenes, including poly(*p*-phenylene), PPV,[39–41] and polythienylenevinylene.[41,42] Chart 10 shows the chemical structures of some side-chain LC conjugated polymers. Cyanobiphenyl (CB) or phenylcyclohexyl (PCH) mesogenic cores were linked to π-conjugated main chain through alkyl spacer. Both smectic and nematic phases were observed for those with PCH mesogenic cores, whereas CB-containing polymers only exhibited smectic mesophase. Taking the example of polymer **P9**, its X-ray diffraction pattern showed two different peaks, sharp and broad ones, at $2\theta = 1.76$ and 19.0 degrees. These two diffraction peaks were evaluated to be 50.2 Å and 4.66 Å, corresponding to an interlayer distance of layered structure and an interchain distance between mesogenic groups, respectively, (as shown in Fig. 11).[41] Besides, polymers show relatively high conductivity of 10^{-3} S/cm under nonoriented condition, which is higher by 3–4 order of magnitude than those of aligned polyacetylene derivatives containing similar mesogens. The results suggest an enhanced coplanarity in the PPV main chains.

Our group also prepared two DP-PPV derivatives (**P12** and **P13** Chart 11) containing LC side groups.[43,44] The thermotropic LC phases of polymers **P12** and **P13** were investigated by differential scanning calorimetry (DSC) and POM. A stable nematic mesophase of polymer **P12** is shown in Figure 12, with a threaded texture observed between 170 and 290 °C. The optical texture of the sample was almost unchanged after quenched to room temperature. In addition to alkylbiphenyl and PCH mesogens, we also reported the synthesis and polarized EL of novel LC PPV copolymers (**P14** in Chart 12) containing laterally attached penta(*p*-phenylene) mesogenes.[45] From DSC thermogram, these polymers show complex thermal behaviors, which contain glass transition, melting, and nematic-isotropic transition. These polymers show microphase separation behavior, which is very common for side-chain LC polymers. The optical micrograph and DSC thermogram of polymer **P14** are shown in Figure 13.

Other example includes PPV derivatives containing LC oxadiazole groups. The mesogenic core comprises heterocyclic 1,3,4-oxadiazole and two adjacent phenyl

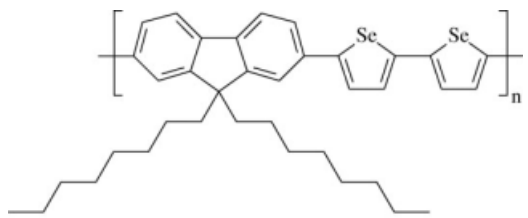

P6

Chart 8. Fluorene-selenophene copolymer.

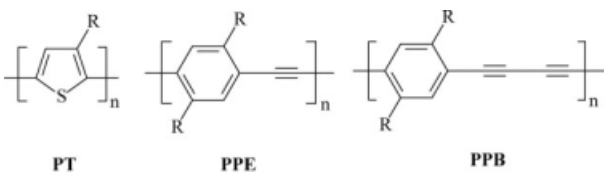

Chart 9. PT, PPE, and PPB polymers.

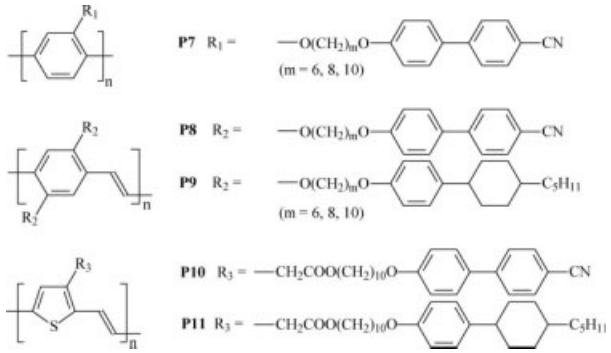

Chart 10. Mesogen-containing conjugated polymers.

rings and is incorporated to PPV main chain through oxymethylene spacer from one side (**P15**) or lateral side, so-called mesogen-jacketed LC polymer (**P16**), as shown in Chart 13.[46,47] For polymer **P15**, although its monomer containing 1,3,4-oxadiazole moiety possessed typical

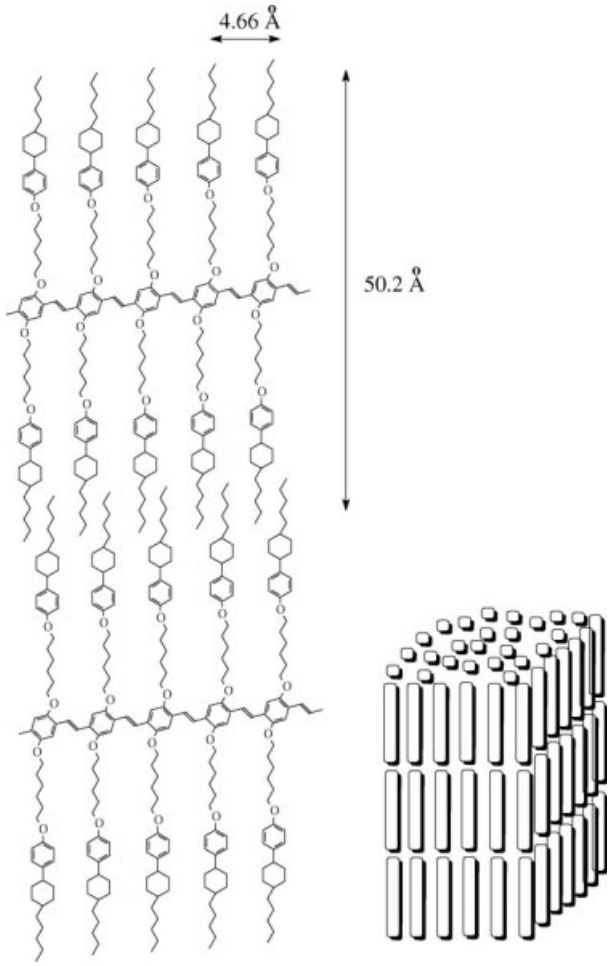

Figure 11. Schematic illustration of the layered structure of polymer **P9**.

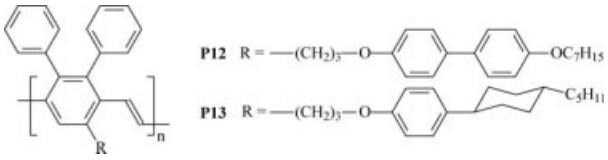

Chart 11. DP-PPV with LC side groups.

schilerene texture to be nematic liquid crystal, the author reported that the resulting polymers showed no LC behavior based on the results of DSC and POM observation. For polymer **P16**, its synthesis, optical, and electrical properties were mentioned; however, no LC properties were discussed in the literature.

A novel side-chain photoresponsive PPV derivative (**P17** in Chart 14) containing hexafluoro-cyclopentene ring was synthesized by Akagi and coworkers[48] as shown in Chart 14. A nematic LC phase was observed in both heating and cooling processes, referring to an enantiotropic nature. The glassy-nematic and nematic-isotropic transition temperatures were further examined to be 95 and >200 °C in the heating process, respectively, whereas nematic-glassy transition temperature was decreased to 85 °C. The photoisomerization of photoresponsive side group can be controlled by exposure of UV or visible light, resulting in open form (fluorenscence) and closed form (quenched fluorescence).

PF derivatives containing mesogenic groups are relatively rare. The most utilizing group is still 1,3,4-oxadiazole. Charts 15–17 show some *co*-PF derivatives with 1,3,4-oxadiazole groups attached on C-9 position of fluorene moiety or 1,3,4-oxadiazole dendritic pendants on the phenylene ring.[49–52] These polymers were mainly developed for the improvement in EL and/or thermal stabilities; no obvious LC properties were mentioned in those previous literatures. Nevertheless, they should be classified as side-chain conjugated polymers as well.

In addition to 1,3,4-oxadiazole mesogens, side-chain LC PF derivatives with laterally attached penta(*p*-phenylene) mesogenes were synthesized and reported by our group.[45] The nematic LC behavior and phase transition temperatures were both well characterized and reported in the previous literature. The chemical structure of those laterally attached side-chain PF derivatives are shown in Chart 18. They possess a wide nematic range from 73 to 81 °C to 258–302 °C, as verified by POM and DSC.

Apart from LC PPV and PF derivatives, a great number of side-chain LC conducting polymers containing mesogenic side chains have also been synthesized and characterized, including PT,[42,48,53–57] polyaniline,[54] and polypyrrole.[54,58,59] The structures of these side-chain LC conducting polymers are given in Charts 19 and 20. Some of them show smectic mesophase in nature, for

Figure 12. Optical texture of polymer **P12** at 175 °C.

example, **P28–P30**, and **P36–P38**, and **P43**, because the alkyl spacer is inserted between rigid main chain and mesogenic side chain; the hindrance from the rigid main chain reduces and mesogenic side chains have the tendency to form layered smectic structure. On the other hand, the others show only nematic phase without adequate alkyl spacer. It should be noted that, for polypyrrole derivatives **P39–P43**, only the polymer with mesogenic groups on both the *N*-position of pyrrole and the methine position in the main chain shows LC properties, that is, no LC mesophase is observed for **P39–P42**. It may be likely that the wide space between neighboring mesogens gives no spontaneous LC aggregation. A typical fan-shape smectic A texture of polymer **P43** is shown in Figure 14.

Recently, conjugated polymers bearing ferroelectric LC groups have drawn much research interest because of their spontaneous polarization in the chiral smectic C (S_C*) phase.[59–64] The chemical structures are shown in Chart 21. Ferroelectricity is required to have a spontaneous polarization that is generated by assembly of dipole moments. It is well known that ferroelectric LC molecules have the ability to respond more quickly to an electric field than formal LC ones. Although these polymers show S_C* phase under certain LC state, however, neither the quick electrosponsive behavior nor the switching function based on polarization inversion has been achieved. This is primarily because of the structurally rigid π-conjugation main chain that prohibits the generation of ferroelectricity using electric field. Figures 15 and 16 show the characteristic chiral smectic fan-shape texture (S_C*) and corresponding WAXS diffraction patterns of polymers **P45** and **P52**, respectively. It is also noted that polyphenylene derivatives **P44–P46** show one or more chiral smectic mesophases, for example, chiral smectic I (S_I*) and chiral smectic J (S_J*) phases for polymer **P45**, whereas only chiral smectic A (S_A*) phase is observed for polymer **P46**.[60] No LC mesophase is found for polymer **P47**, because the neighboring mesogenic groups are too far to form LC aggregate.

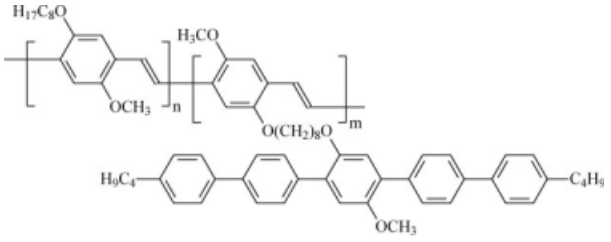

P14

Chart 12. PPV derivative with laterally attached mesogenic groups.

LC CONJUAGTED OLIGOMERS

Conjugated oligomers are those π-conjugated materials with well-defined molecular weight and conjugation length. In many ways, oligomers own better optical properties and are easier to manipulate compared with

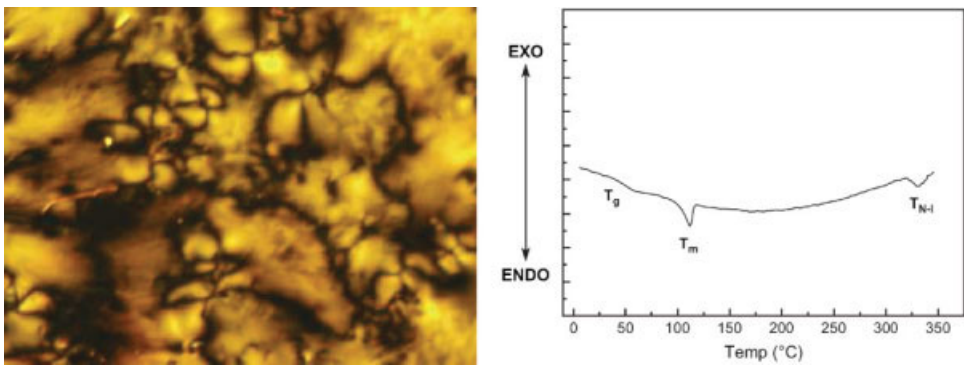

Figure 13. Optical micrograph and DSC thermogram of polymer **P14**.

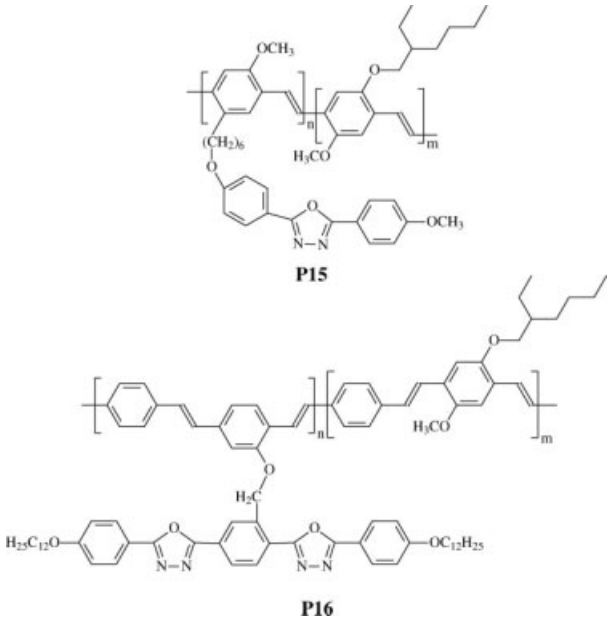

Chart 13. 1,3,4-Oxadiazole-containing PPV derivatives.

their corresponding polymers. Several conjugated oligomers with LC properties have been synthesized to study their photo-physical and self-assembled properties, including oligo(*p*-phenylenevinylene) (OPV),[65–74] oligofluorene,[75–80] and oligo(*p*-phenyleneethynylene).[33,81]

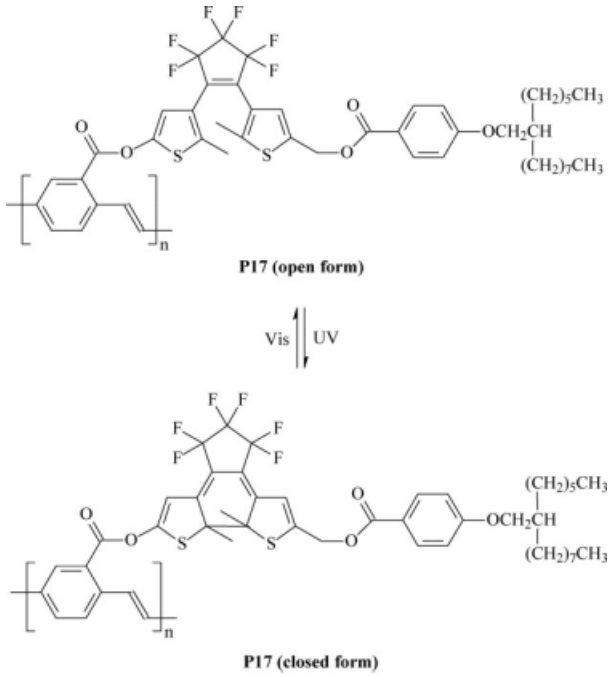

Chart 14. Photoisomerization of polymer **P17** under exposure of UV or visible light.

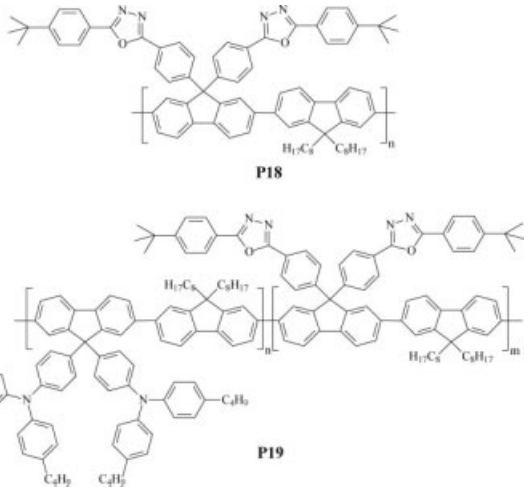

Chart 15. 1,3,4-Oxadiazole-containing *co*-PF derivatives.

POLARIZED EMISSION

Linearly polarized emission has been widely explored for backlight application in liquid crystal displays since 1995. Several techniques have been developed to obtain polarized emission with high polarized ratio, including mechanical stretching,[82,83] direct rubbing,[41,43,48,58,84–86] thermal annealing on polyimide (PI) or poly(3,4-ethylenedioxythiophene) (PEDOT) alignment layer,[19,27,35,45,74–77,86–99] Langmuir-Blodgett film,[14]

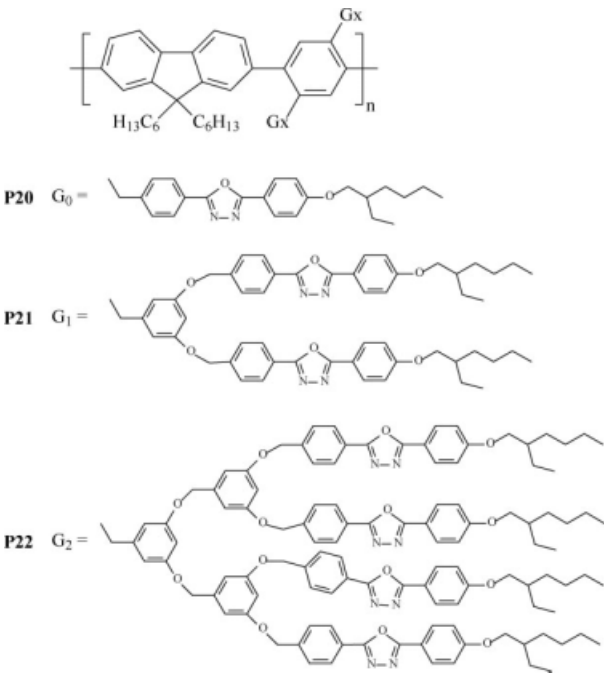

Chart 16. 1,3,4-Oxadiazole-containing *co*-PF derivatives with different generation.

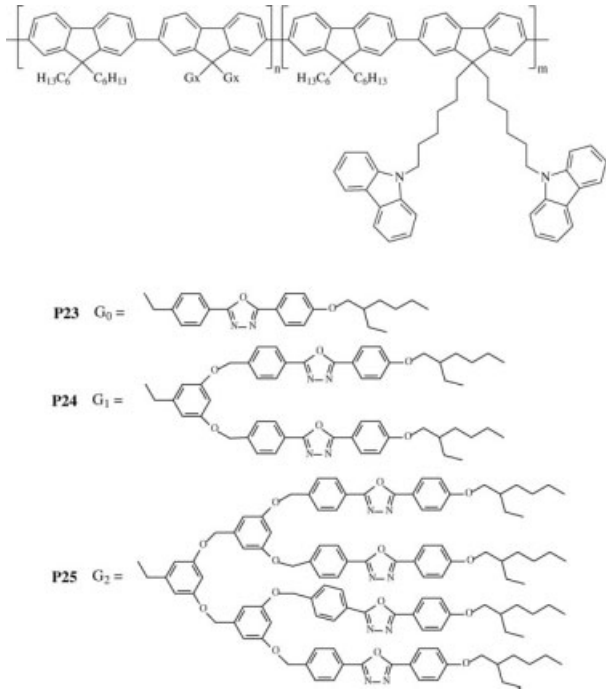

Chart 17. 1,3,4-Oxadiazole-containing *co*-PF derivatives with different generation.

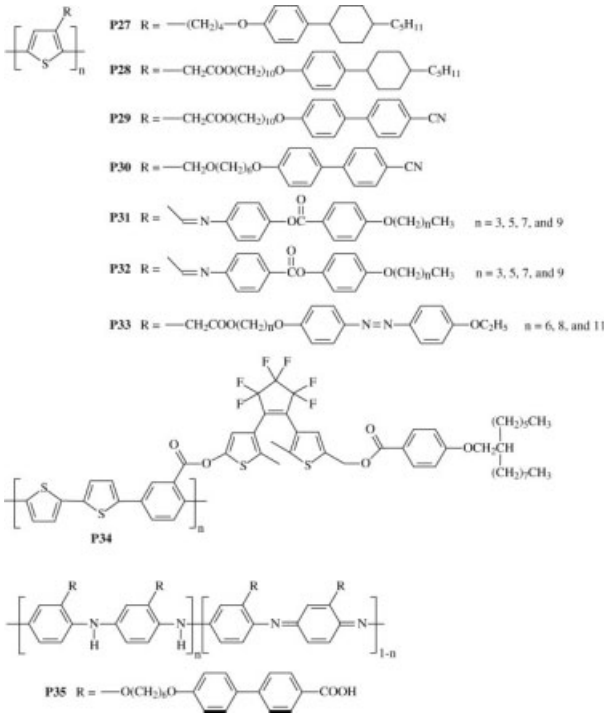

Chart 19. Mesogen-containing side-chain polymers **P27–P35**.

friction transfer,[67,100,101] and other techniques.[40,42,102] For those luminescent materials with no self-organized LC properties, mechanical stretching or the usage of friction transfer of poly(tetrafluoroethylene) (PTFE) could be an alternative way to get polarized emission. Mechanical stretching of pristine polymer film is the simplest way to achieve such kind of polarization emission, because elongation is one of intrinsic properties of polymers. However, the film thickness is usually in μm scale, which is too thick for the fabrication of EL devices. The driving voltage turns out to be very high and luminescent efficiency is thus lowered.[82] Huang and coworkers[83] utilized blending film of PFO/polyethylene (PE) to reach a

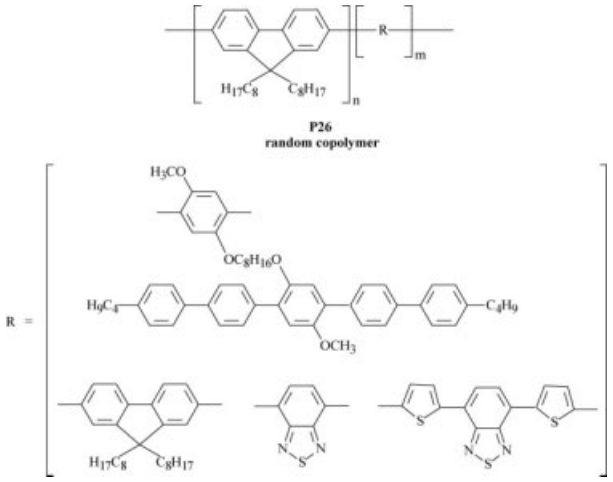

Chart 18. PF derivatives with laterally attached mesogens.

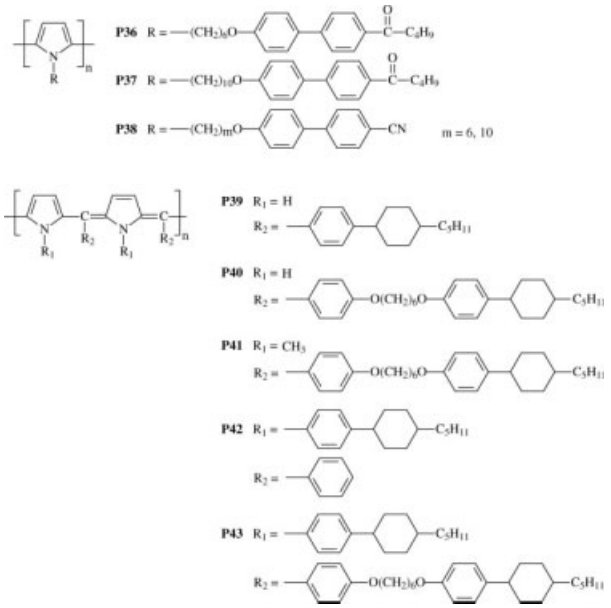

Chart 20. Mesogen-containing polypyrrole derivatives **P36–P43**.

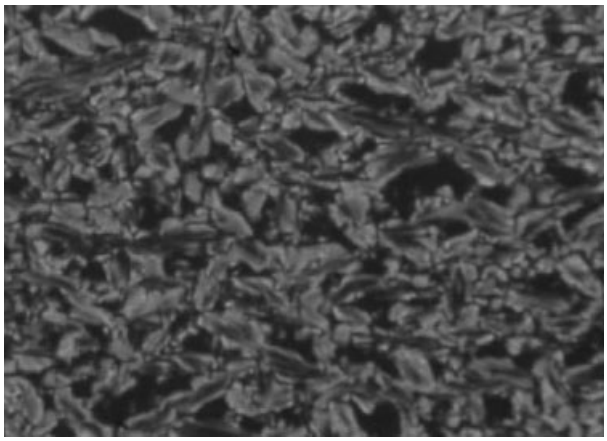

Figure 14. Optical micrograph of polymer **P43**.

very high PL polarization ratio of 58, because of highly elongated characteristic of polymer PE matrix. Furthermore, the vibronic band of the emission in perpendicular direction is also diminished, as shown in Figure 17. The order parameter *S* was estimated to 0.92 from its absorption spectra, indicating a very high degree of orientation. The use of PTFE layer by friction transfer is an alternative way for many kinds of luminescent materials, from small molecules to high-molecular-weight polymers, to obtain polarized emission.[67,100] However, the insulating nature of PE and PTFE restrict their application for the fabrication of polarized EL devices.

Herein, we mainly discuss the polarized emission of LC conjugated materials and report some outstanding results from those previous literatures. The alignment of LC conjugated materials can be achieved by both direct rubbing of the active layer and thermal annealing on additional alignment layer. Both methods mentioned above are always carried out under LC state to fulfill self-organization of LC materials. The direct rubbing of polymer thin film can be proceeded with a glass rod, slide, or a roller covered by nylon cloth. A high polarized ratio of 16 in PL spectra using polymer **P34** as the emissive material was ever achieved.[48] A practical polarized EL device using partially conjugated PPV as the active layer was fabricated with polarized ratio of 12.[85] The emissive intensity in parallel to rubbing direction is usually stronger than that in perpendicular. In some cases, it shows stronger emission in perpendicular to rubbing direction, especially for those side-chain LC conjugated polymers.[41,43] Taking the examples of polymer **P12**, the light emitted from the rubbed film was preferentially polarized perpendicular to the rubbing direction, as shown in Figure 18. This is because rubbing at thermotropic LC phase induces the alignment of mesogenic side groups along the rubbing direction and the alignment of polymer backbones perpendicular to the rubbing direction. As a result, relatively large absorption and emission were observed in the orthogonal direction with respect to the rubbing direction, as shown in Figure 19.

The thermal annealing of light-emitting LC materials is a promising strategy for polarized emission, because it is a noncontact method that can avoid the contamination of emissive layer. The choice of suitable alignment layer is also an important issue. Prerubbed polyimide (PI) is

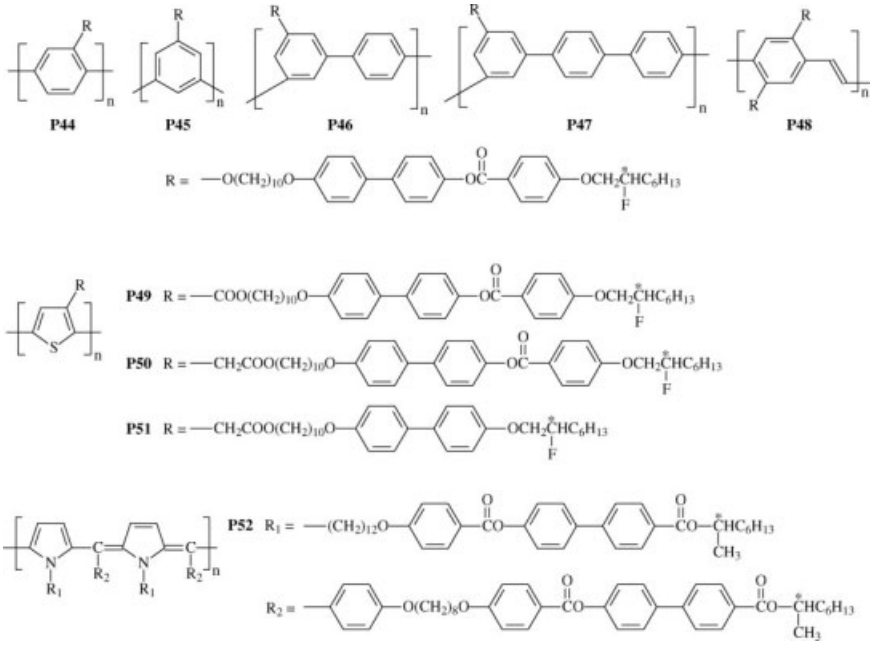

Chart 21. Some conjugated polymers bearing ferroelectric side groups.

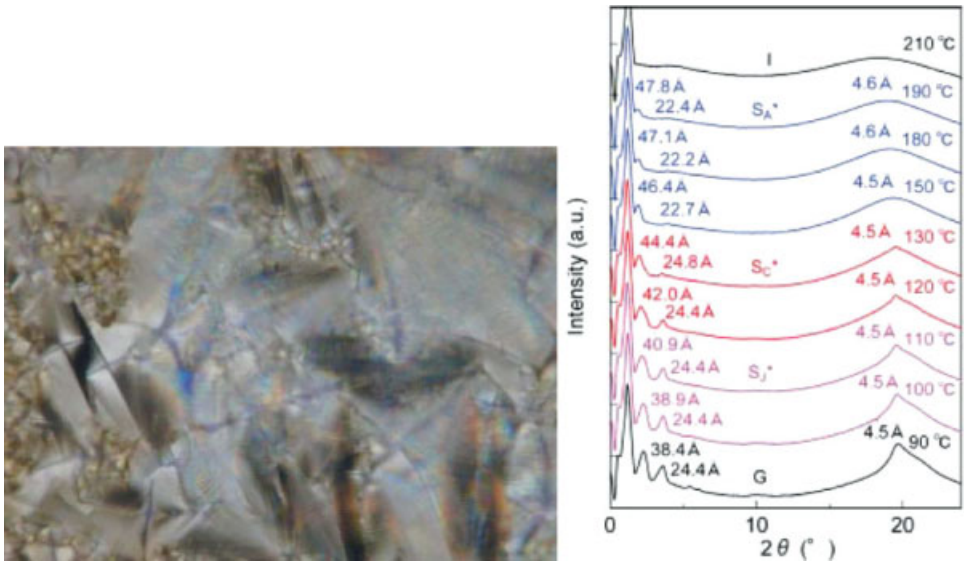

Figure 15. Stripped fan-shape texture (S_C*) of polymer **P45** at 130 °C and its WAXS patterns at different temperatures.

widely used for macroscopic alignment of LC materials. A very high PL polarized ratio of 41 was obtained using heptafluororene oligomer as emissive materials.[78] To increase the conductivity of intrinsically insulating PI, the starburst type (4,4′,4″-tris(1-naphthyl)-*N*-phenylamino)-triphenylamine (ST638) was added in PI.[86,89,90] The structures of commonly used PI and ST638 are shown in Chart 22. Polarized EL devices were fabricated using PF2/6 aligned on rubbed PI/ST638 layer, and a high EL polarized ratio of 15–21 was obtained. However, the luminescent intensity was quite low (45 cd/m^2). Recently, a photoaligned PI film containing azobenzene in the backbone (azoPI) was developed to align PFO.[98,99] A polarized EL device was fabricated with polarization ratio of 29, as shown in Figure 20; the brightness and current efficiency were 700 cd/m^2 and 0.14 cd/A, respectively. In addition, the emissive intensity is stronger in perpendicular to linear UV-exposure direction,

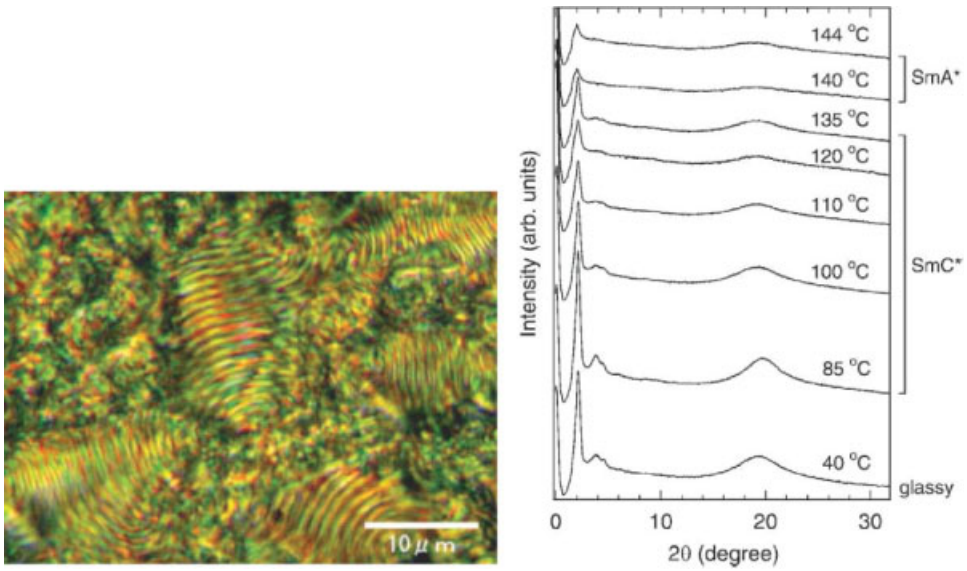

Figure 16. Broken fan-conic texture (S_C*) of polymer **P52** at 100 °C and its WAXS patterns at different temperatures.

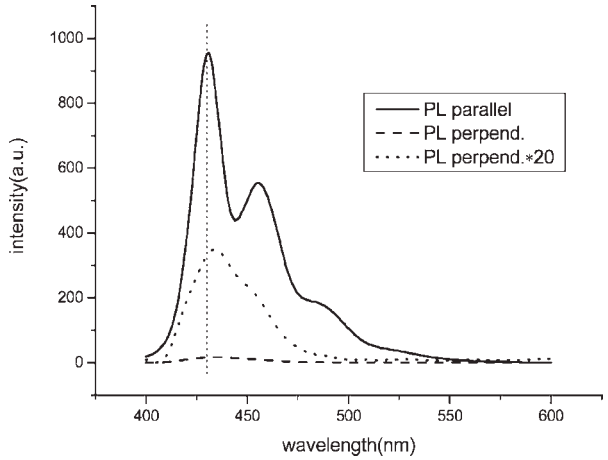

Figure 17. Polarized PL spectra of the PFO/PE elongated blending film.

depending on the isomerization of azobenzene moieties in the main chain.

Other alignment layers include rubbed poly(3,4-ethylenedioxythiophene) (PEDOT),[27,45,75,76] poly(vinylalcohol) (PVA),[67] PPV,[94] poly(*N*-vinylcarbazole) (PVK),[95] and other photoaligned polymers.[77,96,97] PEDOT is well-known for its hole-transporting property and extensively used in light-emitting devices. By rubbing treatment makes it a good candidate for the fabrication of polarized EL devices. A polarized white-light EL device was fabricated by Chen et al.,[76] with high polarization ratio of 15.6 and current efficiency of 4.5 cd/A. Our group also fabricated polarized white-light EL devices using rubbed PEDOT as the alignment layer and copolyfluorene blends as the active layer, with maximum luminescence of 2454 cd/m^2 and polarization ratio of 10.2.[45] Besides, high EL polarization ratio over 25 was ever obtain using rubbed PPV or PVK as the alignment layer.[94,95] Two different side-chain copolymers containing photo-sensitive moieties, that is, coumarin or azobenzene, have also been synthesized for the alignment of LC conjugated materials.[77,96,97] The structures of these two copolymers are shown in Chart 23. The EL polarization ratio of 13 was reported, with maximum luminescence of 100–200 cd/m^2.

The summarized performance of polarized emission of different light-emitting materials and their corresponding alignment techniques are listed in Table 1.

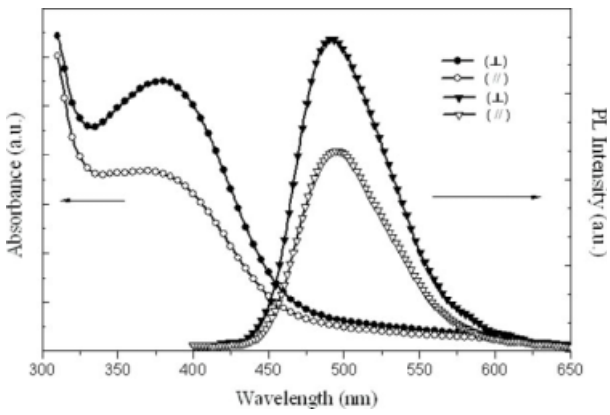

Figure 18. Polarized absorption and PL spectra of polymer **P12**.

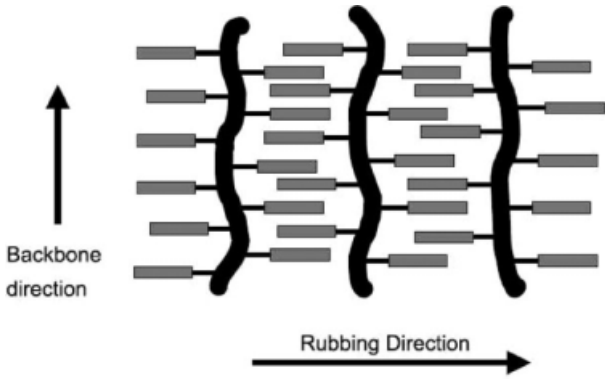

Figure 19. Illustration of the alignment of LC side chains and polymer backbones due to rubbing treatment.

FIELD-EFFECT PROPERTIES

Organic field-effect transistors (OFETs) are generally considered to be potentially low-cost alternatives to amorphous silicon-based technologies for large-area devices. High mobility and on/off ratio are main

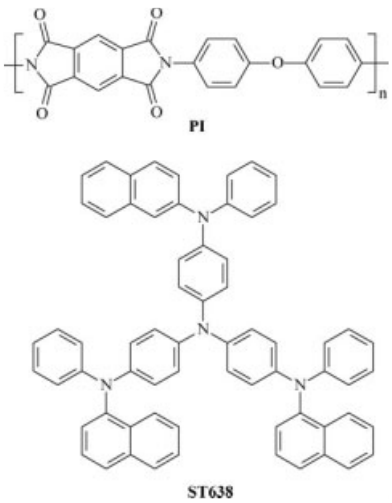

Chart 22. PI and ST638.

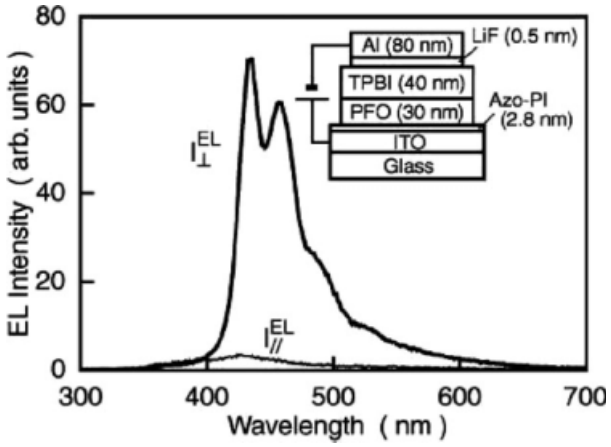

Figure 20. Polarized EL spectra of PFO and azoPI alignment layer. Inset shows the device structure.

concerns to achieve better performance of OFETs. Head-to-tail regioregular poly(3-hexylthiophene) (P3HT) are the most used material for polymer-based OFETs, owing to its intrinsically high mobility of 0.1 cm^2/Vs.[103] The highly ordered crystalline structure of P3HT in thin film is responsible for its high performance in transistor applications. Recently, LC conjugated polymers has attracted progressive attention for their self-organized nature to enhance their mobility, which opens a new trend to high-performance OTFTs. Several LC conjugated polymers have been studied for OFET application, for example, PFTT, PFT2,[104] fluorene-selenophene-based copolymer **P6** (chemical structures are shown in previous section),[28] poly(9,9′-dioctylfluorene-*alt*-benzothiadiazole) (F8BT),[102] poly(3,3‴-didodecylquaterthiophene) (PQT-12),[31] and some fluorene-thiophene copolymers **P55–P57**, as shown in Chart 24. These LC materials showed enhanced charge carrier mobility after aligning the polymer chains on the alignment layer under LC state. A solution-processed OFET device based on **P6** showed a hole mobility of 0.012 cm^2/Vs and a low threshold voltage of −4 V. Mobility of up to 0.18 cm^2/Vs and current on/off ratio of 10^7 were obtained for OFET using PQT-12 as the active layer. The FET characteristics of polymers **P55–P57** are relatively lower, with mobility of 2.8–8.7 $\times$ 10^{-5} cm^2/Vs and current on/off ratio of 2.0–3.0 $\times$ 10^3.

CONCLUSIONS

In this highlight, we have reviewed a great number of main-chain and side-chain LC conjugated polymers and their potential use in polarized EL or FET devices. Main-chain LC conjugated polymers including PPV, PF, PT, and PPE backbone were synthesized. Various side chains can be attached to the conjugated backbone to render it soluble and processable. Commonly used side chains are simple alkyl and alkoxy substituents. These polymers are classified as "hairy rod" polymers and have been found to show nematic phase under LC state. Besides the nematic phase, this kind of polymers usually shows lamellar worm-like morphology. A wide variety of side-chain LC conjugated polymers based on PPV, DP-PPV, PF, PT, polyphenylene, and polypyrrole backbone have also been synthesized. The introduction of mesogenic side chains into such kind of rigid polymer backbone provides this kind of polymers more versatile mesomorphoric properties, including nematic, smectic, and chrial smectic phases.

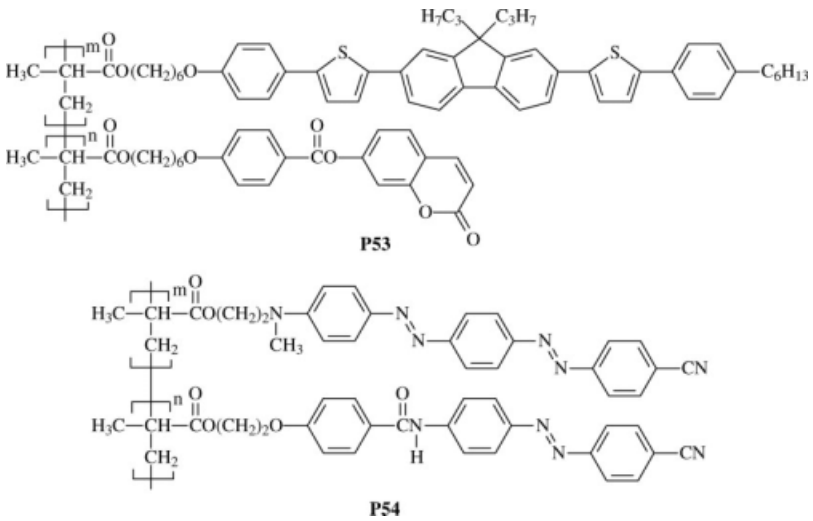

Chart 23. Photoaligned copolymers containing coumarin or azobenzene moieties.

Table 1. Performance of Polarized Emission of Different Light-Emitting Materials and the Applied Alignment Techniques

Materials (λ_{max})	Alignment Technique	P (PL or EL, Direction)	Device Performance	Ref.
PPP (PL 395, EL 524)	Langmuir-Blodgett	3–4 (EL, //)	External Eff. 0.05%	14
P4 (520)	Annealing on rubbed PI	ca. 1.3 (EL, //)	N/A	19
PF copolymers (white)	Annealing on rubbed PEDOT	4.6 (EL, //)	1895 cd/m^2, 0.24 cd/A	27
Dialkoxy-PPB (560)	Annealing in a sandwich cell with rubbing treatment	ca. 2.5 (PL, $\perp$)	N/A	35
P7 (420)	Magnetically forced alignment	ca. 1.4 (PL, $\perp$)	N/A	40
P8 (550)	Direct rubbing	1.2–1.4 (PL, $\perp$)	N/A	41
P28 (560)	Magnetically forced alignment	3.8 (PL, $\perp$)	N/A	42
P12 (500)	Direct rubbing	2.1 (PL, $\perp$)	N/A	43
P14 (588)	Annealing on rubbed PEDOT	2.6 (EL, //)	1337 cd/m^2, 0.33 cd/A	45
P26 (540)	Annealing on rubbed PEDOT	12.4 (EL, //)	1855 cd/m^2, 0.57 cd/A	45
Co-PF blend (white)	Annealing on rubbing PEDOT	10.2 (EL, //)	2454 cd/m^2	45
P34 (575)	Direct rubbing	16 (PL, //)	N/A	48
P38 (510)	Direct rubbing	1.4 (PL, //)	N/A	58
OPV (560)	Annealing on PTFE layer by friction transfer	17.1 (PL, //)	N/A	67
OPV (560)	Annealing on rubbed PVA	13.6 (PL, //)	N/A	67
Oligofluorenes (424)	Annealing on rubbed PEDOT	27.1 (EL, //)	214 cd/m^2, 1.07 cd/A	75
Oligofluorene blend (white)	Annealing on rubbed PEDOT	15.6 (EL, //)	4.5 cd/A	76
Fluorene-thiophene oligomer (500)	Annealing on photoaligned polymer layer	13 (EL, //)	200 cd/m^2	77
Oligofluorenes (417)	Annealing on rubbed PI	41 (PL, //)	N/A	78
PPV (550)	Mechanical stretching	8 (EL, //)	N/A	82
PFO/PE blend (430)	Mechanical stretching	58 (PL, //)	N/A	83
Dinonyloxy-PPV (600)	Direct rubbing	4 (EL, //)	N/A	84
Partial conjugated PPV (511)	Direct rubbing	12 (EL, //)	200 cd/m^2	85
PF2/6 (450)	Annealing on rubbed PI	21 (EL, //)	N/A	86,90
PFO (460)	Annealing on rubbed PI	ca. 6 (PL, //)	N/A	87,88
PF2/6 (477)	Annealing on rubbed PI	15 (EL, //)	45 cd/m^2	89
PF2/6 (450)	Annealing on rubbed PI	12 (PL, //)	N/A	91
PFO (458)	Annealing on rubbed PPV	25 (EL, //)	250 cd/m^2	94
PF (450)	Annealing on rubbed PVK	25.7 (EL, //)	1000 cd/m^2, 0.31 cd/A	95
PF2/6 (445)	Annealing on photoaddressable polymers PAPs	17 (PL, //)	N/A	96
PF2/6 (445)	Annealing on photoaddressable polymer PAPs	13 (EL, //)	100 cd/m^2, 0.66 cd/A	97
PFO (432)	Annealing on photoaligned Azo-PI	30 (PL, $\perp$)	N/A	98
PFO (459)	Annealing on photoaligned Azo-PI	29 (EL, $\perp$)	700 cd/m^2, 0.14 cd/A	99
Dialkoxy-PPV (535)	Annealing on PTFE by friction transfer	4 (EL, //)	N/A	100
PFO (435)	Friction transfer	10 (PL, //)	N/A	101
F8BT (540)	Nanoimprinting	11 (EL, //)	N/A	102

Because of self-organized LC properties of these conjugated polymers, large-domain aligned thin film can be obtained by direct rubbing and/or thermal annealing of the active layer on the rubbed PI or PEDOT surface under LC state. The LC conjugated polymers that are aligned under LC phases to achieve monodomain thin film are the best candidate for the manufacture of highly polarized EL devices. These devices would be particularly useful as backlights for conventional liquid crystal displays (LCDs). This will simplify LCD manufacturing and reduce cost. Furthermore, the LC conjugated polymers also have potential application in organic FET

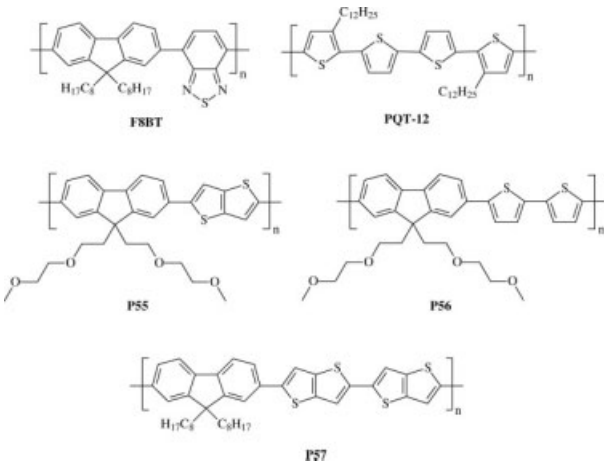

Chart 24. LC conjugated polymers F8BT, PQT-12, and **P55–P57**.

devices. Because the microstructure of the LC conjugated polymers could be controlled by self-organization with the help of an additional alignment layer, the carrier mobility of the FET device can be greatly enhanced.

REFERENCES AND NOTES

1. Kraft, A.; Grimsdale, A. C.; Holmes, A. B. Angew Chem Int Ed 1998, 37, 402–428.
2. Friend, R. H.; Gymer R. W.; Holmes, A. B.; Burroughes, J. H.; Marks, R. N.; Taliani, C.; Bradley, D. D. C.; Dos Santos, D. A.; Brédas, J. L.; Lögdlund, M.; Salaneck, W. R. Nature 1999, 397, 121–128.
3. Bernius, M. T.; Inbasekaran, M.; O'Brien, J.; Wu, W. Adv Mater 2000, 12, 1737–1750.
4. Scherf, U.; List, E. J. W. Adv Mater 2002, 14, 477–487.
5. Neher, D. Macromol Rapid Commun 2001, 22, 1365–1385.
6. Lam, J. W. Y.; Tang, B. Z. J Polym Sci Part A: Polym Chem 2003, 41, 2607–2629.
7. Wessling, R. A.; Zimmerman, R. G. U.S. Patent 3,401,152, 1968.
8. Neef, C. J.; Ferraris, J. P. Macromolecules 2000, 33, 2311–2314.
9. Wan, W. C.; Antoniadis, H.; Choong, V. E.; Razafitrimo, H.; Gao, Y.; Feld, W. A.; Hsieh, B. R. Macromolecules 1997, 30, 6567–6574.
10. Bao, Z.; Chen, Y.; Cai, R.; Yu, L. Macromolecules 1993, 26, 5281–5286.
11. Liao, L.; Pang, Y.; Ding, L.; Karasz, F. E. Macromolecules 2001, 34, 6756–6760.
12. Moratti, S. C.; Cervini, R.; Holmes, A. B.; Baigent, D. R.; Friend, R. H.; Greenham, N. C.; Grüner, J.; Hamer, P. J. Synth Met 1995, 71, 2117–2120.
13. Yu, L.; Bao, Z.; Cai, R. Angew Chem Int Ed 1993, 32, 1345–1347.
14. Cimrová, V.; Remmers, M.; Neher, D.; Wegner, G. Adv Mater 1996, 8, 146–149.
15. Bao, Z.; Amundson, K. R.; Lovinger, A. J. Macromolecules 1998, 31, 8647–8649.
16. Chen, S. H.; Su, A. C.; Chou, H. L.; Peng, K. Y.; Chen, S. A. Macromolecules 2004, 37, 167–173.
17. Chen, S. H.; Su, A. C.; Han, S. R.; Chen, S. A.; Lee, Y. Z. Macromolecules 2004, 37, 181–186.
18. Chen, S. H.; Su, C. H.; Su, A. C.; Chen, S. A. J Phys Chem B 2004, 108, 8855–8861.
19. Shim, H. K.; Hwang, D. H. Thin Solid Films 2002, 417, 166–170.
20. Hsieh, B. R.; Yu, Y.; Forsythe, E. W.; Schaaf, G. M.; Feld, W. A. J Am Chem Soc 1998, 120, 231–232.
21. Olsen, B. D.; Jang, S. Y.; Lüning, J. M.; Segalman, R. A. Macromolecules 2006, 39, 4469–4479.
22. Herguth, P.; Jiang, X.; Liu, M. S.; Jen, A. K.-Y. Macromolecules 2002, 35, 6094–6100.
23. Miteva, T.; Meisel, A.; Knoll, W.; Nothofer, H. G.; Scherf, U.; Müller, D. C.; Meerholz, K.; Yasuda, A.; Neher, D. Adv Mater 2001, 13, 565–570.
24. Chen, S. H.; Su, A. C.; Chen, S. A. J Phys Chem B 2005, 109, 10067–10072.
25. Chen, S. H.; Su, A. C.; Su, C. H.; Chen, S. A. J Phys Chem B 2006, 110, 4007–4013.
26. Lim, E.; Jung, B. J.; Shim, H. K. Macromolecules 2003, 36, 4288–4293.
27. Yao, Y. H.; Kung, L. R.; Hsu, C. S. Jpn J Appl Phys 2005, 44, 7648–7653.
28. Kim, Y. M.; Lim, E.; Kang, I. N.; Jung, B. J.; Lee, J.; Koo, B. W.; Do, L. M.; Shim, H. K. Macromolecules 2006, 39, 4081–4085.
29. Hong, X. M.; Collard, D. M. Macromolecules 2000, 33, 6916–6917.
30. Zhao, N.; Botton, G. A.; Zhu, S.; Duft, A.; Ong, B. S.; Wu, Y.; Liu, P. Macromolecules 2004, 37, 8307–8312.
31. Wu, Y.; Liu, P.; Ong, B. S.; Srikumar, T.; Zhao, N.; Botton, G.; Zhu, S. Appl Phys Lett 2005, 86, 142102.
32. Weder, C.; Sarwa, C.; Montail, A.; Bastiaansen, C.; Smith, P. Science 1998, 279, 835–837.
33. Bunz, U. H. F. Acc Chem Res 2001, 34, 998–1010.
34. Kijima, M.; Kinoshita, I.; Hattori, T.; Shirakawa, H. Synth Met 1999, 100, 61–69.
35. Ozaki, M.; Fujisawa, T.; Fujii, A.; Tong, L.; Yoshino, K.; Kijima, M.; Kinoshita, I.; Shirakawa, H. Adv Mater 2000, 12, 587–589.
36. Kijima, K.; Matsumoto, S.; Kinoshita, I. Synth Met 2003, 135–136, 391–392.
37. Yu, Z. Q.; Liu, J. H.; Yan, J. J.; Liu, X. B.; Liang, D. H.; Lam, J. W. Y.; Dong, Y. P.; Li, Z. C.; Chen, E. Q.; Tang, B. Z. Macromolecules 2007, 40, 8342–8348.

38. Goto, H.; Dai, X.; Ueoka, T.; Akagi, K. Macromolecules 2004, 37, 4783–4793.
39. Oguma, J.; Akagi, K.; Shirakawa, H. Synth Met 1999, 101, 86–87.
40. Park, J. H.; Lee, C. H.; Akagi, K.; Shirakawa, H.; Park, Y. W. Synth Met 2001, 119, 633–634.
41. Akagi, K.; Oguma, J.; Shibata, S.; Toyoshima, R.; Osaka, I.; Shirakawa, H. Synth Met 1999, 102, 1287–1288.
42. Osaka, I.; Goto, H.; Itoh, K.; Akagi, K. Synth Met 2001, 119, 541–542.
43. Li, A. K.; Yang, S. S.; Jean, W. Y.; Hsu, C. S.; Hsieh, B. R. Chem Mater 2000, 12, 2741–2744.
44. Yang, S. H.; Chen, J. T.; Li, A. K.; Huang, C. H.; Chen, K. B.; Hsieh, B. R.; Hsu, C. S. Thin Solid Films 2005, 477, 73–80.
45. Yao, Y. H.; Yang, S. H.; Hsu, C. S. Polymer 2006, 47, 8297–8308.
46. Sun, X.; Li, M.; Liu, D.; Zhang, P.; Tian, W. J Appl Polym Sci 2004, 91, 396–403.
47. Sun, L.; Wang, P.; Jin, H.; Fan, X.; Shen, Z.; Chen, X.; Zhou, Q. F. J Polym Sci Part A: Polym Chem 2008, 46, 7173–7186.
48. Hayasaka, H.; Tamura, K.; Akagi, K. Macromolecules 2008, 41, 2341–2346.
49. Wu, F. I.; Reddy, S.; Shu, C. F.; Liu, M. S.; Jen, A. K.-Y. Chem Mater 2003, 15, 269–274.
50. Shu, C. F.; Dodda, R.; Wu, F. I.; Liu, M. S.; Jen, A. K.-Y. Macromolecules 2003, 36, 6698–6703.
51. Wu, C. W.; Sung, H. H.; Lin, H. C. J Polym Sci Part A: Polym Chem 2006, 44, 6765–6774.
52. Wu, C. W.; Tsai, C. M.; Lin, H. C. Macromolecules 2006, 39, 4298–4305.
53. Toyoshima, R.; Nirita, M.; Akagi, K.; Shirakawa, H. Synth Met 1995, 69, 289–290.
54. Brown, J. W.; Foot, P. J. S.; Gabaston, L. I.; Ibison, P.; Prevost, A. Macromol Chem Phys 2004, 205, 1823–1828.
55. Radhakrishnan, S.; Somanathan, N.; Narasimhaswamy, T. J Polym Sci Part B: Polym Phys 2008, 46, 1463–1477.
56. Zhao, X.; Hu, X.; Zheng, P. J.; Gan, L. H.; Lee, C. K. P. Thin Solid Films 2005, 477, 88–94.
57. Zhao, X.; Wang, M. Eur Polym Mater 2006, 42, 247–253.
58. Abe, S.; Kijima, M.; Shirakawa, H. Mol Cryst Liq Cryst 2001, 365, 247–253.
59. Goto, H.; Akagi, K. J Polym Sci Part A: Polym Chem 2005, 43, 616–629.
60. Suda, K.; Akagi, K. J.; Polym Sci Part A: Polym Chem 2008, 46, 3591–3610.
61. Oguma, J.; Dai, X.; Akagi, K. Mol Cryst Liq Cryst 2001, 365, 331–338.
62. Dai, X. M.; Narihiro, H.; Goto, H.; Akagi, K.; Yokoyama, H. Synth Met 2001, 119, 397–398.
63. Goto, H.; Dai, X.; Narihiro, H.; Akagi, K. Macromolecules 2004, 37, 2353–2362.
64. Goto, H.; Akagi, K.; Dai, X.; Narihiro, H. Ferroelectrics 2007, 348, 149–153.
65. Maddux, T.; Li, W.; Yu, L. J Am Chem Soc 1997, 119, 844–845.
66. Zhu, W.; Li, W.; Yu, L. Macromolecules 1997, 30, 6274–6279.
67. Lauhof, M. W.; Benning, S. A.; Kitzerow, H. S.; Vill, V.; Scheliga, F.; Thorn-Csányi, E. Synth Met 2007, 157, 222–227.
68. Amrutha, S. R.; Jayakannan, M. Macromolecules 2007, 40, 2380–2391.
69. Pisula, W.; Tomovic, Z.; Wegner, M.; Graf, R.; Pouderoijen, M. J.; Meijer, E. W.; Schenning, A. P. H. J. J Mater Chem 2008, 18, 2968–2977.
70. Wang, H.; Wang, H. H.; Urban, V. S.; Littrell, K. C.; Thiyagarajan, P.; Yu, L. J Am Chem Soc 2000, 122, 6855–6861.
71. Mori, T.; Watanabe, T.; Minagawa, K.; Tanaka, M. J Polym Sci Part A: Polym Chem 2005, 43, 1569–1578.
72. Hulvat, J. F.; Sofos, M.; Tajima, K.; Stupp, S. I. J Am Chem Soc 2005, 127, 366–372.
73. Gu, T.; Accorsi, G.; Armaroli, N.; Guillon, D.; Nierengarten, J. F. Tetrahedron Lett 2001, 42, 2309–2312.
74. Precup-Blaga, F. S.; Schenning, A. P. H. J.; Meijer, E. W. Macromolecules 2003, 36, 565–572.
75. Culligan, S. W.; Geng, Y.; Chen, S. H.; Klubek, K.; Vaeth, K. M.; Tang, C. W. Adv Mater 2003, 15, 1176–1180.
76. Chen, A. C. A.; Culligan, S. W.; Geng, Y.; Chen, S. H.; Klubek, K. P.; Vaeth, K. M.; Tang, C. W. Adv Mater 2004, 16, 783–788.
77. Aldred, M. P.; Contoret, A. E. A.; Farrar, S. R.; Kelly, S. M.; Mathieson, D.; O'Neill, M.; Tsoi, W. C.; Vlachos, P. Adv Mater 2005, 17, 1368–1372.
78. Chi, C.; Lieser, G.; Enkelmann, V.; Wegner, G. Macromol Chem Phys 2005, 206, 1597–1609.
79. Yu, X. F.; Lu, S.; Ye, C.; Li, T.; Liu, T.; Liu, S.; Fan, Q.; Chen, E. Q.; Huang, W. Macromolecules 2006, 39, 1364–1375.
80. Zhang, X.; Bu, L.; Qu, Y.; Wang, L.; Geng, Y.; Wang, F. J Mater Chem 2009, 19, 399–408.
81. Yatabe, T.; Suzuki, Y.; Kawanishi, Y. J Mater Chem 2008, 18, 4468–4477.
82. Lemmer, U.; Vacar, D.; Moses, D.; Heeger, A. J.; Ohnishi, T.; Noguchi, T. Appl Phys Lett 1996, 68, 3007–3009.
83. He, B.; Li, J.; Bo, Z.; Huang, Y. Macromolecules 2005, 38, 6762–6766.
84. Hamaguchi, M.; Yoshino, K. Appl Phys Lett 1995, 67, 3381–3383.
85. Jandke, M.; Strohriegl, P.; Gmeiner, J.; Brütting, W.; Schwoerer, M. Adv Mater 1999, 11, 1518–1521.
86. Miteva, T.; Meisel, A.; Grell, M.; Nothofer, H. G.; Lupo, D.; Yasuda, A.; Knoll, W.; Kloppenburg, L.;

Bunz, U. H. F.; Scherf, U.; Neher, D. Synth Met 2000, 111–112, 173–176.
87. Grell, M.; Bradley, D. D. C.; Inbasekaran, M.; Woo, E. P. Adv Mater 1997, 9, 798–802.
88. Bradeley, D. D. C.; Grell, M.; Grice, A.; Tajbakhsh, A. R.; O'Brien, D. F.; Bleyer, A. Opt Mater 1998, 9, 1–11.
89. Grell, M.; Knoll, W.; Lupo, D.; Meisel, A.; Miteva, T.; Neher, D.; Nothofer, H. G.; Scher, U.; Yasuda, A. Adv Mater 1999, 11, 671–675.
90. Nothofer, H. G.; Meisel, A.; Miteva, T.; Neher, D.; Forster, M.; Oda, M.; Lieser, G.; Sainova, D.; Yasuda, A.; Lupo, D.; Knoll, W.; Scherf, U. Macromol Symp 2000, 154, 139–148.
91. Bauer, C.; Urbasch, G.; Giessen, H.; Meisel, A.; Nothofer, H. G.; Neher, D.; Scherf, U.; Mahrt, R. F. Chem Phys Chem 2000, 1, 142–146.
92. Song, M. H.; Wenger, B.; Friend, R. H. J App Phys 2008, 104, 033107.
93. Marusaki, M.; Ikame, S.; Kobawashi, A.; Naito, H. Thin Solid Films 2008, 516, 2392–2395.
94. Whitehead, K. S.; Grell, M.; Bradley, D. D. C.; Jandke, M.; Strohriegl, P. Appl Phys Lett 2000, 76, 2946–2948.
95. Chung, S. F.; Wen, T. C.; Chou, W. Y.; Guo, T. Z. Jpn J Appl Phys 2006, 45, L60–L63.
96. Sainova, D.; Zen, A.; Nothofer, H. G.; Asawapirom, U.; Scherf, U.; Hagen, R.; Bieringer, T.; Kostromine, S.; Neher, D. Adv Funct Mater 2002, 12, 49–57.
97. Yang, X. H.; Neher, D.; Lucht, S.; Nothofer, H.; Güntner, R.; Scherf, U.; Hagen, R.; Kostromine, S. Appl Phys Lett 2002, 81, 2319–2321.
98. Sakamoto, K.; Usami, K.; Uehara, Y. Appl Phys Lett 2005, 87, 211910.
99. Sakamoto, K.; Miki, K. Appl Phys Lett 2007, 91, 183509.
100. Chen, X. L.; Bao, Z.; Sapjeta, B. J.; Lovinger, A. J.; Crone, B. Adv Mater 2000, 12, 344–347.
101. Misaki, M.; Ueda, Y.; Nagamatsu, S.; Yoshida, Y.; Tanigaki, N.; Yase, K. Macromolecules 2004, 37, 6926–6931.
102. Zheng, Z.; Yim, K. H.; Saifullah, M. S. M.; Welland, M. E.; Friend, R. H.; Kim, J. S.; Huck, W. T. S. Nano Lett 2007, 7, 987–992.
103. Sirringhaus, H.; Brown, P. J.; Friend, R. H.; Nielsen, M. M.; Bechgaard, K.; Langeveld-Voss, B. M. W.; Spiering, A. J. H.; Janssen, R. A.; Meijer, E. W.; Herwig, P.; de Leeuw, D. M. Nature 1999, 401, 685–688.
104. Lim, E.; Jung, B. J.; Lee, J.; Shim, H. K.; Lee, J. I.; Yang, Y. S.; Do, L. M. Macromolecules 2005, 38, 4531–4535.
105. Lim, E.; Kim, Y. M.; Lee, J. I.; Jung, B. J.; Cho, N. S.; Lee, J.; Do, L. M.; Shim, H. K. J Polym Sci Part A: Polym Chem 2006, 44, 4709–4721.